Spatial self-correction of the spotted structure of high-power pulsed laser radiation at optical breakdown on atmospheric paths

N.N. Bochkarev, A.M. Kabanov, and V.A. Pogodaev

V.E. Zuev Institute of Atmospheric Optics,
Siberian Branch of the Russian Academy of Sciences, Tomsk

Propagation of high-power laser radiation in haze has been studied *in situ*. It was shown that using the acoustic response it is possible to detect remotely changes in the laser intensity over the beam cross section and along the propagation path. The absence of plasma centers (PCs) on the propagation path at laser radiation energy density sufficient for optical breakdown at aerosol particles was observed for the first time.

Introduction

Design and development of lasers generating high-power coherent radiation, as well as results of investigation of such radiation interaction with various media stimulated the search for new solutions of some practical problems. The list of new technologies using high-power lasers extends permanently. One of the fields of interest is the fast input of laser radiation energy into a given spatial point far remote from the source of radiation. This field includes such prospective technologies as the control for lightning trajectory, wireless energy transportation, remote cutting of large polluted objects, determination of elemental composition of aerosol atmospheric pollutants, and so on.

As an example, consider the actively developed technology of the laser guidance of the lightning discharge along a given trajectory. Now we know four main physical problems (in addition to many purely technical problems), without solution of which the existing pilot systems can hardly become the routine. It is necessary:

1) to understand the lightning initiation processes;

2) to know peculiarities of laser radiation propagation through the atmosphere (efficiency of transportation);

3) to be able to form efficiently a highly ionized channel in the atmosphere;

4) to elaborate the method of setting the time of the laser turn-on.

Among these problems,[1–3] the second and the third ones concern nonlinear atmospheric optics, that is, include the problem of propagation of high-power laser radiation (HPLR) through the atmosphere with accounting for the whole variety of nonlinear effects appearing at HPLR interaction with atmospheric substances. This is important to a great extent for the fourth problem as well.

When solving the problem of influence of atmospheric factors on the laser radiation extinction, the prediction of atmospheric influence on characteristics of some or other laser systems is considered in most cases. Optical characteristics of the atmosphere are described with the use of their statistical models being average distributions for various regions or seasons.[4]

The specificity in consideration of atmospheric factors in field studies and tests of high-power laser systems is that the used instrumentation, without distorting the laser beam, is to diagnose and determine the influence of quite specific weather and optical characteristics of an atmospheric channel existing during the experiment.[5,6] Such formulation of the problem faces certain difficulties connected, in particular, with the real-time estimation of optical characteristics of aerosols and, especially, their dynamics in the process of their interaction with the high-power radiation.[5]

In Ref. 7, the coefficient of absorption of optical radiation in the real atmosphere was measured for the first time, based on the phenomenon of sound generation upon the atmosphere heating by an amplitude-modulated CO_2 laser beam. Significant spatiotemporal fluctuations of the absorption coefficient have been observed, and the results obtained show aerosol to be responsible for this effect. For atmospheric nonlinear optics, these fluctuations are among decisive factors deteriorating the laser beam coherence.

Note that the influence of aerosol on the absorption coefficient of an atmospheric channel of laser radiation propagation was observed[7] with the use of low-power radiation (cw 550-W radiation modulated with a frequency of 4–16 kHz). In this case, the structure and integrity of aerosol particles were not disturbed.[5]

Experimental investigations of the optoacoustic effect upon change in the phase state of a particulate

substance under controllable laboratory and field conditions[8-12] have shown that parameters of acoustic signals, generated in the channel of high-power laser radiation, are determined by both characteristics of absorbed radiation and optical, thermophysical, and acoustic properties of the absorbing medium. Depending on the power degree of the laser radiation action on the atmospheric substance and according to commonly accepted terminology, the most significant mechanisms of optoacoustic sound generation can be divided into the following parts: thermooptcal; regular evaporation and explosive boiling-up of liquid aerosol particles; and optical breakdown (so-called interaction regimes). The same mechanisms determine the level of extinction of laser radiation, initiating their appearance in the atmospheric channel. Determination of main mechanisms of laser radiation extinction in various weather situations is the necessary condition for correct interpretation of the obtained results and correct planning of works connected with optimization of laser radiation transportation through the atmosphere.

Underline that the main advantage of the optical method of the sound generation is its remote character. The possibility to receive an acoustic response from a medium at any azimuth and zenith angles of orientation of the laser beam optical axis is limited in distance mostly by the level of the HPLR energy transformed into the energy of the acoustic source.

The acoustic energy evolved by explosion of an individual fog droplet does not exceed $\sim 10^{-10}$ J at laser radiation energy density ($\lambda = 10.6$ μm) within $2-6$ J/cm² [Ref. 13]. At the same time, an individual plasma center (PC) initiated by an aerosol particle of roughly the same size evolves $\sim 10^{-3}$ J. This value significantly exceeds the level evolved by a water droplet explosion. The number of plasma centers formed in the high-power laser beam is determined by the beam energy, as well as aerosol concentration and microstructure.

Just the acoustic method of determining the parameters of laser radiation interaction with aerosol particles during propagation along ground atmospheric paths under various weather conditions allowed us to remotely show these parameters to be identical to the parameters of the same processes taking place under controllable laboratory conditions.[13] Therefore, on the one hand, we can use fully the available collected laboratory database on measurements of high-power radiation interaction with aerosol particles to reliably interpret the degree of extinction of laser radiation energy in the real atmosphere. On the other hand, this method, without distorting the integrity of the laser beam, allows monitoring of the beam energy and spatial parameters (energy distribution over the cross section).

The cross section of laser beams can change significantly during propagation in the atmosphere. It should be kept in mind that the changes concern both the beam aperture due to initial divergence (or due to focusing to a given distance) and the centroid position due to regular refraction and self-induced optical inhomogeneities in the medium.

Thus, having determined remotely the regime of high-power radiation interaction with atmospheric substance, we can estimate the radiation energy density at a particular section of the propagation path.

This paper presents the results of experimental investigation of the laser beam "breathing" effect, observed for the first time, during propagation in the actual atmosphere, as well as the absence of plasma centers at the path at laser radiation energy density exceeding the optical breakdown threshold of the atmosphere. These effects were detected from the acoustic response of the atmospheric channel of laser radiation propagation.

Instrumentation and procedure of combined measurements

The experimental system can be conditionally divided into three groups:

– the source of laser radiation, the aligning systems, instrumentation for recording of radiation parameters at the beginning of the path (energy, pulse length and shape);

– the atmospheric path (orography, position with respect to the wind rose), instruments for measurement of standard meteorological parameters: temperature, pressure, air humidity, wind speed and direction, as well as instrumentation for measurement of the aerosol particle concentration and size distribution function, meteorological visibility range, and the structural constant of refractive index fluctuations C_n^2;

– detectors of atmospheric response to the action of high-power laser radiation (acoustic and optical), radiation energy, time profile of radiation pulse.

The laser beam geometry was kept unchanged $F/a_0 = 900$ (F is the focal length of the transmitting mirror telescope, forming the radiation beam with the initial radius a_0). In experiments, we used the pulse CO_2 laser radiation of microsecond length, close to axially symmetric one.

Without going into detail of the whole system, let us characterize thoroughly the propagation path and detectors of acoustic and optical responses. The path was oriented with respect to wind rose along the predominant direction of air masses. In this way, we minimized the influence of air mass motion across the beam on optical characteristics of the laser beam propagation channel. The path length for the experimental data under consideration was ~ 0.5 km.

The disperse composition of aerosol was determined by an AZ-5 type counter of aerosol particles. Experiments were conducted in the presence of haze in the propagation path. The obtained aerosol particle size distribution functions are given in Fig. 1.

It is seen the evolution in the disperse composition of haze (curves 1 and 2) with increase of humidity (Table). Note that the haze was formed based on the summer light haze. The relative humidity of air, characterizing the first laser shot, achieved 93% during an hour, from 23:23 (curve 1) to 00:28 (curve 2).
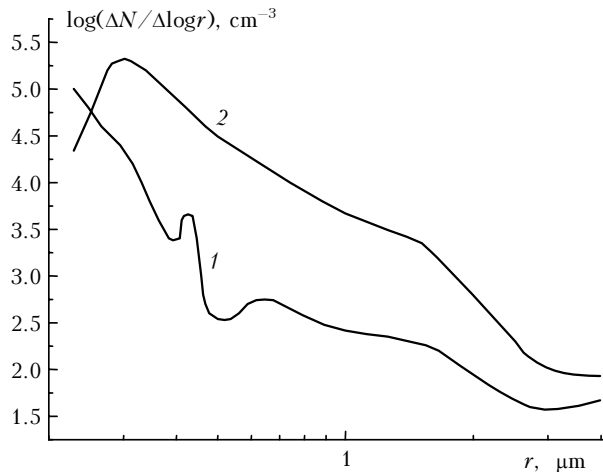
Fig. 1. Influence of humidity on the size distribution function of haze particles.

The aerosol component of the atmospheric extinction coefficient undisturbed by high-power laser radiation was determined according to Ref. 14. The composition of the gas component was calculated from meteorological data according to Ref. 15.

The detector of the atmospheric acoustic response to HPLR operated as follows. The microphone with a passband of 20 kHz and a dynamic range of ~54 dB was set at ~1 m far from the beam axis. In compilation of the "soundtrack" archive, a 12-bit ADC with a discretization frequency of 36 kHz was used.

The laser pulse length was much shorter than the sound travel time across the beam.

Physical foundations of the acoustic method as an indicator of the process of HPLR interaction with aerosol particles are described in Ref. 5. The technique of recording and decoding of soundtracks formed by plasma centers (PCs) initiated by HPLR action on individual aerosol particles is considered in detail in Ref. 16. The problems of the processing of recorded acoustic signals and their possible distortions by the atmosphere and the surface are discussed in Ref. 17. Dissipative, diffraction, and nonlinear distortions of the shape of acoustic signals generated in the HPLR channel are predicted and taken into consideration in the algorithm of the Atmospheric Optoacoustics, developed by us. The algorithm retrieves initial characteristics of acoustic signals, using available meteorological data, experimental geometry, and multichannel spectral transformations.

The optical response of the atmospheric channel is understood as visualization of new properties of the HPLR (for example, long laser spark (LLS)) propagation channel, or redistribution of radiation intensity over the channel cross section due to refractive distortions. The response should be recorded either on photography (LLS) or in the form of the corresponding replica (change in the screen relief). As a material for replicas (screen), we used strong cardboard sheets. The corresponding screens were set in the way of the radiation beam behind a bolometric transmission-type energy meter at the end of the path.

Table. Meteorological and optical conditions characterizing optical properties of the atmospheric optical channel to the moment of laser shot

Shot number	Shot time	RH, %	t, °C	S_m, km	V, m/s	α_{H_2O}, km^{-1}	α_{CO_2}, km^{-1}	α_a, km^{-1}	E_f, J/cm^2	T
1	23:23	91	12.7	8.5	3/6	0.172	0.066	0.185		
2	23:30	92	12.6	8.0	»	0.174	»	0.196		
3	23:34	»	12.5	»	»	0.181	»	»		
4	00:18	93	11.9	6.7	2/5	0.169	0.065	0.235		
5	00:28	»	11.8	6.1	2	0.165	»	0.258	13	0.92
6	00:32	»	»	5.8	»	»	»	0.271	17.5	0.56
7	00:37	»	11.7	5.4	»	0.164	»	0.291	16	0.59
8	00:41	»	»	5.1	»	»	»	0.308	12	0.75
9	00:44	»	11.6	5.0	»	0.163	0.064	0.314	14	0.5
10	00:48	»	»	4.7	»	»	»	0.334	11.5	0.52
11	00:52	»	11.5	4.4	1	0.164	»	0.357	9	0.67
12	00:57	»	11.4	4.1	»	0.160	»	0.383	10.5	0.48
13	01:03	»	11.3	»	»	0.112	»	»	9	0.89
14	01:38	95	10.5	5.0	2	0.153	0.063	0.314	16	0.47
15	01:44	»	»	»	»	»	»	»	14	0.29
16	02:21	96	10.3	4.3	»	»	»	0.365	8.5	0.47
17	02:28	»	10.2	4.1	»	0.152	»	0.383	7	0.43
18	02:33	»	»	3.9	»	»	»	0.403	6	0.42
19	02:37	»	10.1	3.7	»	0.150	»	0.425	7	0.29
20	02:41	»	10.0	3.5	»	0.149	0.062	0.449	5.5	0.55

N o t e s . Pressure $P = 740$ mm Hg; $C_n^2 \sim 10^{-16}$ cm$^{-2/3}$ did not vary during measurements; RH and t are the relative humidity and temperature of air; S_m and V are the meteorological visibility range and wind velocity; α_{H_2O} is the coefficient of continual absorption of radiation with $\lambda = 10.6$ μm by water vapor; α_{CO_2} is the coefficient of resonance absorption by carbon dioxide; α_a is the aerosol extinction coefficient; E_f is the laser radiation energy density averaged over the beam cross section at the focal region with neglected atmospheric extinction; T is the path transmittance.

The same procedure was also used at the path beginning (before entrance to the telescope) for qualitative monitoring of the initial radiation intensity distribution over the beam cross section. If necessary, Dacron attenuators were used. The character of distortion of the surface layers in replicas obtained under field conditions was reconstructed in laboratory measurements with the corresponding control for energy level of the acting radiation.

According to Ref. 18, radiation of CO_2 lasers, equal to ~2 J/cm^2, is sufficient for printing noticeable replicas on the cardboard. Analysis of beam images recorded at the beginning of the path has shown that the structure and shape of the beam are reproduced satisfactorily in the case, when the conditions of radiation formation and the laser working mixture are unchanged. This allows us to be sure that, despite the beam structure cannot be recorded simultaneously at different parts of the path, the comparison and analysis of beam images, obtained at different points of the path for different shots, are true provided weather parameters change insignificantly during the measurements.

For digital processing of the obtained replicas, beam images from the cardboard were photographed by a digital camera and inputted in computer. To remove the influence of spatial inhomogeneities caused by radiation intensity fluctuations,[19] correlation analysis of an image was performed by the contour, symmetric relative to the beam center. The inhomogeneous energy distribution over the beam cross section determines the correlation function behavior, stipulating the appearance of characteristic spatial scales of its variation.
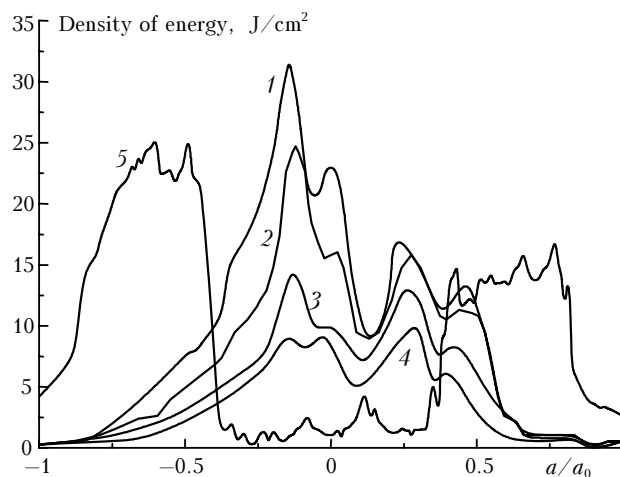

Fig. 2. Energy distribution over the beam cross section.

In the beam image recorded at the path beginning, there are three scales in the region of positive correlation: with radii of 1.5 mm, 1.2 cm, and the scale of positive correlation (correlation radius), which is determined by the size and quality of the beam as a whole. The first two correlation scales are clearly seen in the beam image recorded on a photographic film from the replica at the beginning

of the path and on the densitogram obtained for this case with a microdensitometer (Fig. 2, curve 5).

In this case, the microdensitogram was a qualitative reference for calculations.

Results and discussion

It was noted in Ref. 17 that in addition to pulses from individual PCs, the acoustic response of the HPLR propagation channel includes a thermoacoustic signal, which carries a replica of radiation energy distribution over the beam cross section, that is, it can serve an indicator of energy inhomogeneity of the beam. The physical pattern of the process of radiation absorption (resonance absorption at the carbon dioxide molecular transition $10^00{-}00^01$ and simultaneous thermalization of the laser energy absorbed by water vapor) and corresponding changes in thermodynamic characteristics of air are described in Ref. 20. The experimental part of Ref. 20 was carried out in a wide range of weather conditions. The air temperature during experiments varied from -7 to 25°C, and the humidity ranged from 2 to 15 g/m^3. Direct bolometric measurements were performed simultaneously with acoustic recording of inhomogeneity of energy distribution over the beam cross section. It has been shown that the acoustic method can reconstruct quite well the intensive and large details of the distribution, their relative sizes, distances between them, and relative orientation.

Note that acoustic recording in Ref. 20 was carried out in a particular cross section of a beam. To do this, several acoustic detectors lying in the plane of this cross section were needed, which was possible only on ground horizontal paths. Naturally, the remote character of such measurements was lost.

Figure 2 shows an example of energy distribution over the HPLR beam cross section reconstructed with the use of the Atmospheric Optoacoustic software (curves $1{-}4$). The distance d along the path to the focusing system is 400 m.

In this case, the thermoacoustic signal generated by the HPLR channel was recorded by one detector located 30 m far from the beam axis. The cylindrical divergence of an acoustic wave and the sound absorption were taken into account. It is seen that one-position recording is quite sufficient for estimation of energy fullness of homogeneity over the beam cross section. As the radiation energy decreases and the beam diameter is unchanged, the inhomogeneity of energy distribution over the cross section decreases. A significant transformation of the transversal structure of laser beam upon propagation of a path section should be noted. The level of energy fullness in the region of the paraxial gap, observed in the laser beam before the focusing system (curve 5) increases significantly upon propagation of the path section (curves $1{-}4$).

Figure 3 exemplifies the process of LLS formation upon HPLR propagation through the haze atmosphere.

The values of acoustic pressure obtained by averaging over shots Nos. 5–13 (see the Table): $P_{PC,max}$

and $P_{PC,min}$ are amplitudes of acoustic pressure generated by the largest and smallest PCs, respectively.
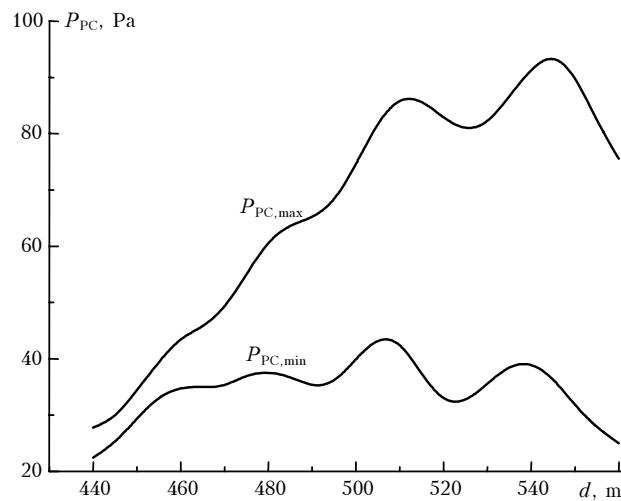

Fig. 3. Amplitude-spatial distribution of the acoustic pressure fields formed along the beam propagation path.

Averaging was performed over all plasma centers, starting from $d = 440$ m, lying on the sequential parts of the 5 m long path. The range of possible acoustic pressures generated by individual PCs lay between the curves corresponding to $P_{PC,max}$ and $P_{PC,min}$. The laser radiation was focused at a distance of 530–540 m. The optical breakdown threshold at a distance of 440 m from the focusing system was 20–25 J/cm². Stable longitudinal fluctuations of $P_{PC,max}$ and $P_{PC,min}$ with a spatial scale of ~30 m are indicative of longitudinal fluctuations of laser radiation energy density in the beam and characterize the longitudinal variability of the energy density distribution over the beam cross section. Density waves, formed in the process of interaction of aerosol and radiation concentrated in the fine structure of the laser beam, are optical inhomogeneities capable of changing in time phase relations between convergent beam filaments. This can cause transformation of the beam spatial structure.

Changes in medium density resulting from interaction of high-power radiation with aerosol particles look like compression – depression waves, formed in the region of radiation intensity fall and propagating over the beam cross section. At pulse lengths $\tau_p \geq \tau = R/C_{ac}$ (R is the size of beam filament, C_{ac} is the acoustic speed), the medium response is significantly nonlocal and depending on the field distribution at previous time instants. Consequently, at the size of high-energy filaments, existing in the beam at the beginning of the propagation path, $\tau \sim 10^{-6}$ s. This can be followed by a change of converging waves and, consequently, field structure in the beam. The field contracts to the near-axis zone (averaging over the beam cross section) with simultaneous increase of spatial modulation of the radiation intensity. The processing of replicas obtained in the focal region of the beam,

demonstrates intensity spikes of ~1–3 mm spaced by ~5–7 mm. The number of small-scale intensity spikes in the focal region is much greater than that at the beginning of the path. We failed to estimate reliably the radiation energy density in small-scale spikes, because of strong and various damages of replicas by them. Such damages start at laser radiation energy density of ≥ 80 J/cm². In this case, contrast boundaries of large-scale regions of energy inhomogeneity disappear completely. The radiation energy distribution over the laser beam cross section (neglecting small-scale spikes) acquires a super-Gaussian form.

Analysis of the data obtained has revealed an interesting peculiarity from the viewpoint of dependence of the path transmittance T on the laser radiation energy density and weather conditions. The values of T for shots Nos. 5–13 differ considerably from those for shots Nos. 14–20. The rate of fall of the dependence $T(E_f)$ is 0.018 for the first group at the increase of energy deposition into the medium by 1 J/cm²; and 0.006 for the second group. It is seen in Table that densities of the laser radiation initial energy at the entrance into the propagation medium differ insignificantly, while the transmittance sensitivity to the propagation conditions appeared in the process of HPLR interaction with the atmosphere for the identical values of E_f in both groups is three times higher for the first group.

According to the Table, there was a half-hour break for technical maintenance of the experimental system between shots of the first and second groups. Data differ radically by the presence of PCs on the path for the first group and their absence for the second group. Underline that the instrumentation for acoustic detection and the laser radiation energy meters operated in the standard mode. The meters of laser radiation energy were checked for spread of their parameters relative to the initial one after termination of a series of shots. No deviations were found.

The main processes of HPLR interaction with aerosol particles at the haze path are evaporation of the aerosol liquid phase, leading to clearing-up of the interaction channel, and the threshold formation of PCs on solid particles.[21] These two processes determine transmission properties of the atmospheric channel, depending on the laser pulse energy, as well as the aerosol concentration and microstructure, which, in turn, significantly depend on the air humidity.

In the situation under consideration, the ratio τ_f/τ_0 changed from 0.3 to 2.28 for the first group of data and from 1.62 to 3.47 for the second group. Here, τ_0 is the initial optical depth of the path calculated from meteorological data; τ_f is the optical depth of the path by the moment of the laser radiation termination. It is seen that the presence of PCs on the path can lead both to clearing up and turbidity of the atmospheric channel. For the second group, a stable increase in turbidity is observed.

Conclusion

Thus, the qualitative investigation of the intensity distribution over the HPLR beam cross section using

the replica technique under field conditions has shown that the radiation intensity transforms significantly during a pulse. At some points of the cross section, the radiation intensity increases locally by several times.

Acoustic accompaniment of *in situ* investigations at an arbitrary or hard-to-reach path points allows the process of intensity transformation to be assessed remotely without the use of acoustic tomography in various optical-meteorological situations in the atmosphere and at critical values of HPLR intensity for appearance of nonlinear optical effects in its interaction with atmospheric aerosol.

The acoustic support of our investigations has allowed us to observe reliably, for the first time, the absence of PCs at HPLR energy densities, which are sufficient for optical breakdown at aerosol particles. This underlines the urgency of the analysis (proposed in Ref. 22) of the possible improvement conditions for HPLR stable transmission in the atmosphere.

References

1. E.M. Bazelyan and Yu.P. Raizer, Uspekhi Fiz. Nauk **170**, No. 7, 753−769 (2000).
2. A.A. Starikov and Yu.A. Rezunkov, J. Opt. Technol. **66**, No. 3, 181−182 (1999).
3. Shigeaki Uchida, Yoshinori Shimada, Hirohiko Yasuda, Shinji Motokoshi, Chiyoe Yamanaka, Tatsuhiko Yamanaka, Zen-ichiro Kawasaki, and Koji Tsubakimoto, J. Opt. Technol. **66**, No. 3, 199−202 (1999).
4. V.M. Osipov, N.F. Borisova, O.M. Galantseva, and V.V. Tsukanov, J. Opt. Technol. **66**, No. 3, 958−964 (1999).
5. Yu.E. Geints, A.A. Zemlyanov, V.E. Zuev, A.M. Kabanov, and V.A. Pogodaev, *Nonlinear Optics of Atmospheric Aerosol* (SB RAS Publishing House, Novosibirsk, 1999), 260 pp.
6. V.P. Aksenov, V.A. Banakh, V.V. Valuev, V.E. Zuev, V.V. Morozov, I.N. Smalikho, and R.Sh. Tsvyk, *High-Power Laser Beams in Randomly Inhomogeneous Atmosphere* (SB RAS Publishing House, Novosibirsk, 1998), 341 pp.
7. V.V. Kolosov and A.V. Kuzikovskii, Opt. Atmos. **1**, No. 3, 57−60 (1988).
8. N.N. Bochkarev, N.P. Krasnenko, V.A. Pogodaev, and A.E. Rozhdestvenskii, in: *Abstracts of Reports at 3rd All-Union Meeting on Laser Radiation Propagation in Disperse Medium* (Obninsk, 1985), Part 3, pp. 42−45.
9. N.N. Bochkarev, A.A. Zemlyanov, N.P. Krasnenko, V.A. Pogodaev, and A.E. Rozhdestvenskii, Pis'ma v Zh. Techn. Fiz. **14**, No. 1, 25−29 (1988).
10. N.N. Bochkarev, Yu.E. Geints, A.A. Zemlyanov, A.M. Kabanov, and N.P. Krasnenko, Opt. Atm. **1**, No. 10, 111−112 (1988).
11. N.N. Bochkarev, N.P. Krasnenko, and Yu.M. Sorokin, Atmos. Oceanic Opt. **3**, No. 6, 513−527 (1990).
12. Yu.V. Akhtyrchenko, N.N. Bochkarev, Yu.P. Vysotskii, O.V. Garin, V.E. Zuev, Yu.D. Kopytin, N.P. Krasnenko, A.I. Kuryapin, V.L. Mironov, V.A. Pogodaev, Vl.V. Pokasov, and B.G. Sidorov, in: *Abstracts of Reports at 8th All-Union Symposium on Laser and Acoustic Sounding of the Atmosphere* (Tomsk, 1984), Part 2, pp. 114−118.
13. N.N. Bochkarev, Yu.E. Geints, A.A. Zemlyanov, A.M. Kabanov, and V.A. Pogodaev, Atmos. Oceanic Opt. **11**, No. 7, 602−607 (1998).
14. V.L. Filippov, V.P. Ivanov, and N.V. Kolobov, *Dynamics of Optical Weather* (Kazan State University Press, Kazan, 1986), 157 pp.
15. T.V. Blakhovskaya and A.A. Mitsel', in: *Laser Radiation Propagation in Absorbing Medium* (IAO SB RAS, Tomsk, 1982), pp. 67−80.
16. N.N. Bochkarev, A.A. Zemlyanov, A.M. Kabanov, and V.A. Pogodaev, Atmos. Oceanic Opt. **14**, No. 12, 1046−1049 (2001).
17. N.N. Bochkarev, A.M. Kabanov, and V.A. Pogodaev, Atmos. Oceanic Opt. **16**, No. 9, 750−755 (2003).
18. H.G. Heard, *Laser Parameter Measurements Handbook* (Wiley, New York, 1968).
19. V.L. Mironov, *Laser Beam Propagation in the Turbulent Atmosphere* (Nauka, Novosibirsk, 1981), 246 pp.
20. Vl.V. Pokasov, V.V. Vorob'ev, A.S. Gurvich, A.S. D'yakov, and V.S. Pryanichnikov, Atmos. Oceanic Opt. **3**, No. 8, 792−798 (1990).
21. A.A. Zemlyanov, G.A. Mal'tseva, and V.A. Pogodaev, Opt. Atmos. **2**, No. 6, 609−614 (1989).
22. V.A. Pogodaev, Atmos. Oceanic Opt. **10**, No. 10, 709−711 (1997).